

# Palladium Phosphino-Iminolate Complexes as Metalloligands for Coinage Metals: A Versatile, Ambivalent Behavior<sup>‡</sup>

Nicola Oberbeckmann-Winter,<sup>†</sup> Pierre Braunstein,<sup>\*,†</sup> and Richard Welter<sup>§</sup>

Laboratoire de Chimie de Coordination and Laboratoire DECMET, UMR 7513 CNRS, Université Louis Pasteur, 4 Rue Blaise Pascal, F-67070 Strasbourg Cédex, France

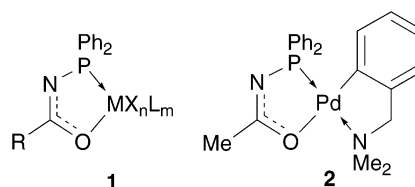
Received March 4, 2005

Reactivity studies with the bis-chelated Pd(II) phosphino-iminolate complex [Pd(dmba)( $\kappa^2$ -P,O-PPh<sub>2</sub>N $\rightleftharpoons$ C( $\rightleftharpoons$ O)Me)] (**2**) (dmba = orthometalated dimethylbenzylamine) have shown that it readily reacts as a metalloligand with electrophilic complexes of the coinage metals, selectively via the nitrogen atom of the P,O chelate. After examining its reaction with AgOTf (OTf = SO<sub>3</sub>CF<sub>3</sub>), which afforded the first 1-D coordination polymer containing Ag–Pd bonds, [Ag(**2**)OTf]<sub>n</sub> (**3**·OTf), we have examined and compared its reactions with H<sup>+</sup>, Au(PPh<sub>3</sub>)<sup>+</sup>, [AuCl(THT)], [Au(THT)BF<sub>4</sub>], and [Cu(NCMe)<sub>4</sub>]BF<sub>4</sub>. Depending on the nature of the electrophilic metal reagent used, the interaction between the iminolate N atom of **2** and the electrophile can be formally described as a dative bond involving its lone pair, which would formally place the positive charge of the complex more on the coinage metal, or as a more covalent interaction resulting in an increased carbon–oxygen bond order and thus in the positive charge being more localized on the Pd(II) center. In the former case, the metalloligand formally behaves as a two-electron, L-type donor, whereas in the latter, as a one-electron, X-type donor ligand. This ambivalent behavior explains the formation of the heterobimetallic complexes [Pd(dmba)( $\kappa^2$ -P,O-PPh<sub>2</sub>NC(O)Me)}AuCl] (**6**) and [Pd(dmba)( $\kappa^2$ -P,O-PPh<sub>2</sub>NC(O)Me)}Au(PPh<sub>3</sub>)OTf] ([Au(PPh<sub>3</sub>)(**2**)OTf] or [Pd(dmba)( $\kappa^2$ -P,O-PPh<sub>2</sub>NC(O)Me)}Au(THT)BF<sub>4</sub>] (**7**·BF<sub>4</sub>), respectively. Double substitution of the d<sup>10</sup> metal center by **2** afforded the Pd/Au/Pd and Pd/Cu/Pd heterotrimeric complexes [Pd(dmba)( $\kappa^2$ -P,O-PPh<sub>2</sub>NC(O)Me)}<sub>2</sub>Au]BF<sub>4</sub> (**8**·BF<sub>4</sub>) and [Pd(dmba)( $\kappa^2$ -P,O-PPh<sub>2</sub>NC(O)Me)}<sub>2</sub>Cu]BF<sub>4</sub> (**9**·BF<sub>4</sub>), respectively. The complexes **2**, **5**·OTf, **6**, **7**·BF<sub>4</sub>, **8**·BF<sub>4</sub>·2CH<sub>2</sub>Cl<sub>2</sub>, and **9**·BF<sub>4</sub> have been structurally characterized by X-ray diffraction.

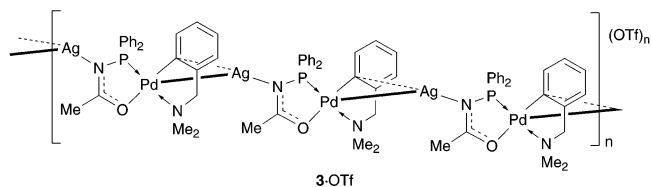
## Introduction

Some transition metal complexes can behave as metalloligands and are increasingly used as well-defined building blocks for the stepwise construction of polynuclear complexes. This approach is particularly interesting in heterometallic chemistry, where it allows a more rational structural design based on the predictable behavior of the components. However, selective and high-yield syntheses require a good understanding of the reactivity of these building units toward a range of metal reagents. We have recently found that air-stable Pd(II) phosphino-iminolate complexes of type **1** readily react with electrophilic metal complexes to form hetero- or polynuclear complexes upon chemoselective metal coordination at the sp<sup>2</sup>-hybridized nitrogen atom of the P,O-chelate.<sup>1</sup>

This results in new ( $\mu$ -P,N)-bridged heterometallic complexes, with retention of the planar coordination



geometry at the nitrogen. The reaction of the palladium phosphino-iminolate complex [Pd(dmba)( $\kappa^2$ -P,O-PPh<sub>2</sub>N $\rightleftharpoons$ C( $\rightleftharpoons$ O)Me)] (**2**) (dmba = orthometalated dimethylbenzylamine) with AgOTf (OTf = SO<sub>3</sub>CF<sub>3</sub>) afforded the first 1-D coordination/organometallic polymer containing Ag–Pd bonds [Ag(**2**)OTf]<sub>n</sub> (**3**·OTf), which opens an unprecedented access to ordered structures with alternating metals based on heterodimetallic units.<sup>1</sup>



We therefore became interested in exploring further the reactivity of complexes of type **1** toward electrophilic

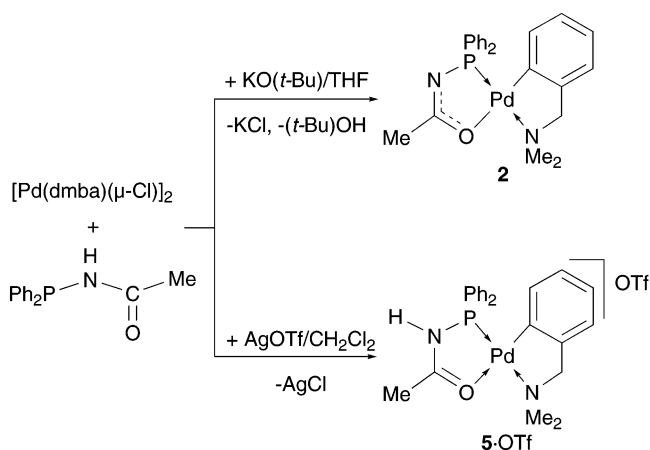
<sup>‡</sup> Dedicated to Prof. Dr. H. Schmidbaur in recognition of his brilliant career and major contributions to chemistry.

<sup>\*</sup> To whom correspondence should be addressed. E-mail: braunst@chimie.u-strasbg.fr. Fax: (+33)3-9024-1322.

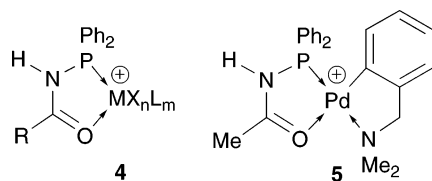
<sup>†</sup> Laboratoire de Chimie de Coordination (UMR 7513 CNRS).

<sup>§</sup> Laboratoire DECMET (UMR 7513 CNRS).

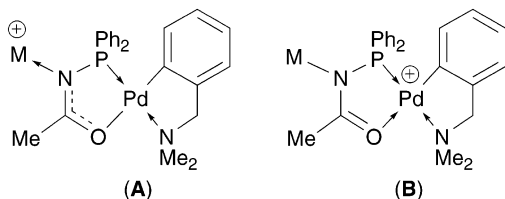
(1) Braunstein, P.; Frison, C.; Oberbeckmann-Winter, N.; Morise, X.; Messaoudi, A.; Bénard, M.; Rohmer, M.-M.; Welter, R. *Angew. Chem., Int. Ed.* **2004**, *43*, 6120.

**Scheme 1. Improved, One-Pot Syntheses of 2 and 5·OTf**


complexes of the coinage metals. Whereas protonation of **1** quantitatively leads to a cationic phosphine complex of type **4** containing formally a  $\text{C}=\text{O}$  double bond and a dative interaction between this oxygen donor and the metal, the situation is less straightforward with metal complexes, even with those that are isolobal with the proton.<sup>1</sup>



Thus, an interesting question arises about the formal description of the interaction between the iminolate N atom of **1** and a metal cation: is it formally going to be a dative bond involving its lone pair, as in a type **A** structure, or a more covalent interaction, as in **B**, resulting in an increased carbon–oxygen bond order and in the positive charge of the complex being more localized on the Pd(II) center than on the coinage metal? Intermediate situations between these limiting forms are also conceivable.



In the present study, we have used as metalloligand of type **1** the complex  $[\text{Pd}(\text{dmba})(\kappa^2\text{-P,O-PPh}_2\text{NHC(O)Me})]$  (**2**)<sup>1</sup> and explored its reactivity toward Au(I) and Cu(I) electrophiles, which led to new P,N-bridged heterometallic complexes.

**Results and Discussion**

Since  $[\text{Pd}(\text{dmba})(\kappa^2\text{-P,O-PPh}_2\text{NHC(O)Me})]$  (**2**)<sup>1</sup> was the main precursor complex for the present studies, an improved, one-step synthesis was desirable (Scheme 1), which is detailed in the Experimental Section.

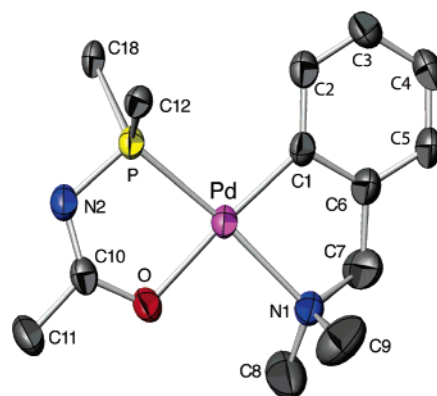


**Figure 1.** ORTEP view of the structure of  $[\text{Pd}(\text{dmba})(\kappa^2\text{-P,O-PPh}_2\text{NHC(O)Me})]$  (**2**) with the atom numbering scheme. Only the *ipso* aryl carbon atoms on P are shown for clarity. Thermal ellipsoids enclose 50% of the electron density. Selected bond distances (Å) and angles (deg): Pd–C(1) 1.998(4), Pd–O 2.106(3), Pd–N(1) 2.134(4), Pd–P 2.219(1), P–N(2) 1.685(4), N(2)–C(10) 1.299(6), C(10)–C(11) 1.514(6), C(10)–O 1.293(5); C(1)–Pd–O 176.2(2), C(1)–Pd–N(1) 82.6(2), O–Pd–N(1) 93.6(1), C(1)–Pd–P 103.1(1), O–Pd–P 80.67(9), N(1)–Pd–P 173.1(1), Pd–P–N(2) 103.6(2), N(2)–C(10)–O 126.9(4), C(10)–O–Pd 114.9(3).

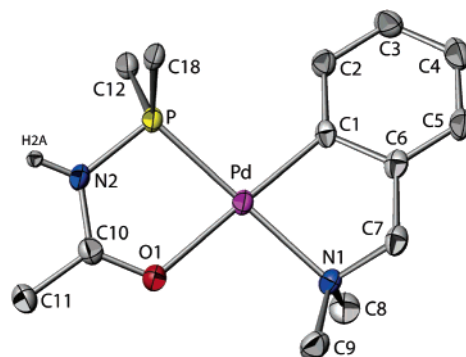


**Figure 2.** ORTEP view of the structure of  $[\text{Pd}(\text{dmba})(\kappa^2\text{-P,O-PPh}_2\text{NHC(O)Me})]^+$  in **5·OTf** with the atom numbering scheme. Only the *ipso* aryl carbon atoms on P are shown for clarity. Thermal ellipsoids enclose 50% of the electron density. Selected bond distances (Å) and angles (deg): Pd–C(1) 1.990(2), Pd–O(1) 2.142(2), Pd–N(1) 2.130(2), Pd–P 2.2164(6), P–N(2) 1.699(2), N(2)–C(10) 1.347(3), C(10)–O(1) 1.251(3), C(10)–C(11) 1.485(4); C(1)–Pd–N(1) 82.09(9), C(1)–Pd–O(1) 179.07(7), N(1)–Pd–O(1) 97.12(7), C(1)–Pd–P 98.42(7), N(1)–Pd–P 176.45(6), O(1)–Pd–P 82.40(5), Pd–P–N(2) 99.47(8), N(2)–C(10)–C(11) 117.6(2), N(2)–C(10)–O(1) 120.8(2), C(10)–O(1)–Pd 116.9(2).

The crystal structure of this complex has been determined and compared with that of the corresponding protonated complex  $[\text{Pd}(\text{dmba})(\kappa^2\text{-P,O-PPh}_2\text{NHC(O)Me})\text{-OTf}]$  (**5·OTf**), whose original synthesis<sup>2</sup> has also been improved (see Scheme 1 and Experimental Section) (Figures 1 and 2, Table 1). The structure of the latter is very similar to that of  $[\text{Pd}(\text{dmba})(\kappa^2\text{-P,O-PPh}_2\text{NHC(O)Me})\text{BF}_4]$  (**5·BF<sub>4</sub>**).<sup>3</sup> Hydrogen bonding was found between the NH function and either a fluorine atom ( $\text{BF}_4$ ) or a oxygen atom (OTf) of the counterion, but in contrast to the disordered  $\text{BF}_4$  anion which develops

(2) Braunstein, P.; Frison, C.; Morise, X.; Adams, R. D. *J. Chem. Soc., Dalton Trans.* **2000**, 2205.

(3) Morise, X.; Braunstein, P.; Welter, R. *Inorg. Chem.* **2003**, *42*, 7752.

**Table 1. Comparison of Bond Lengths and IR Vibration Frequencies between Related Iminolato Complexes**

	Pd–O	C–O	C–N	P–N	$\nu(\text{NC}+\text{CO})$
<b>2</b>	2.106(3)	1.293(5)	1.299(6)	1.685(4)	1501s <sup>a</sup>
<b>5</b> <sup>+</sup>	2.142(2)	1.251(3)	1.347(3)	1.699(2)	1604s <sup>a</sup>
[AuCl( <b>2</b> )] ( <b>6</b> )	2.118(4)	1.265(6)	1.347(6)	1.701(4)	1506s <sup>b</sup>
[Au(THT)( <b>2</b> )]BF <sub>4</sub> ( <b>7</b> ·BF <sub>4</sub> )	2.108(5)	1.236(9)	1.342(9)	1.704(6)	1509s <sup>b</sup>
[Au(PPh <sub>3</sub> )( <b>2</b> )] <sup>+</sup> <sup>c</sup>	2.121(5)	1.273(9)	1.353(9)	1.700(6)	1517s <sup>a</sup>
[Au( <b>2</b> ) <sub>2</sub> ]BF <sub>4</sub> ( <b>8</b> ·BF <sub>4</sub> )	2.136(4)/2.134(4)	1.250(6)/1.255(6)	1.344(7)/1.328(7)	1.708(5)/1.709(5)	1508s <sup>b</sup>
[Cu( <b>2</b> ) <sub>2</sub> ]BF <sub>4</sub> ( <b>9</b> ·BF <sub>4</sub> )	2.124(3)/2.113(3)	1.261(5)/1.264(5)	1.333(6)/1.336(6)	1.712(4)/1.716(4)	1492s <sup>b</sup>
[{Ag( <b>2</b> )}OTf] <sub>n</sub> ( <b>3</b> ·OTf) <sup>c</sup>	2.103(3)	1.286(5)	1.342(6)	1.701(4)	1496s <sup>a</sup>
[Ag( <b>2</b> ) <sub>2</sub> ]OTf <sup>c</sup>	2.102(4)/2.110(4)	1.260(7)/1.276(7)	1.318 (7)/1.337(7)	1.690(5)/1.706(5)	1494s <sup>b</sup>

<sup>a</sup> Recorded in CH<sub>2</sub>Cl<sub>2</sub>. <sup>b</sup> Recorded as KBr disk. <sup>c</sup> From ref 1.

three NH···F interactions (av 2.88 Å), the OTf anion was not disordered and only one NH···O interaction is present (2.78(1) Å, N–H–O = 177.4(3)°). In both cases, the Pd,P,N,C,O chelate ring is almost planar (maximum deviation out of this plane of 0.033(2) Å for N(2) in **2** and of 0.026(1) Å for O(1) in **5**·OTf, respectively). The nitrogen atom N(2) in **5**·OTf has a planar coordination environment (sum of the three bond angles of 359.0(2)°). It is interesting to compare the degree of electronic delocalization within the five-membered P,O chelate rings. A delocalized  $\pi$ -system is present in **2**, as deduced from the values for the N(2)–C(10) and C(10)–O bond distances of 1.299(6) and 1.293(5) Å, respectively, which contrasts with the more localized bonding situation in **5**·OTf, for which the corresponding values are 1.347(3) and 1.251(3) Å, respectively (Table 1), and clearly indicates a pronounced C=O double bond character, consistent with the IR data (see below). In both complexes, the P–N(2) distances are similar and in the normal range for single bonds, suggesting that the P atom in **2** is not significantly involved in the electronic delocalization. This is also consistent with the similarity of the <sup>31</sup>P{<sup>1</sup>H} NMR chemical shift, 81.9 and 80.4 ppm in CDCl<sub>3</sub> for **2** and **5**·OTf, respectively. We have found previously that coordination of a metal center, such as Ag<sup>+</sup> or Au(PPh<sub>3</sub>)<sup>+</sup>, to the iminolate nitrogen N(2) of **2** to give **3**·OTf and [Au(PPh<sub>3</sub>)(**2**)]OTf, respectively, results in a partial relocalization of the electronic system,<sup>1</sup> which emphasizes the similarities between these cationic metal fragments and H<sup>+</sup>, although significant differences are observed in the IR spectra of the complexes in the  $\nu(\text{NC}+\text{CO})$  region (see Table 1). Whereas the IR absorption of **5**·OTf at 1604 cm<sup>-1</sup> corresponds to the  $\nu(\text{C}=\text{O})$  vibration of a coordinated ketone, the values found around 1500–1520 cm<sup>-1</sup> for the di- or trinuclear complexes are much more similar to that of 1501 cm<sup>-1</sup> assigned to  $\nu(\text{N}=\text{C}+\text{C}=\text{O})$ , characteristic of the delocalized system in **2**. This apparent contradiction has already been noted before in the case of the metalation of phosphino-enolate Pd(II) complexes and was suggested to be due to the mass and/or electronic effect of the heavy d<sup>10</sup> metal compared to the proton.<sup>4,5</sup> The bond distances and angles within the Pd(dmab) moiety are similar to those found in the literature.<sup>3,6</sup>

To examine whether complex **2** prefers to coordinate to a metal center formally as a donor (L-type) or a covalent (X-type) metalloligand, a helpful textbook formalism that facilitates bookkeeping of electrons around the metals, it was reacted in a mixture of toluene/CH<sub>2</sub>Cl<sub>2</sub> with 1 equiv of [AuCl(THT)], which

contains the labile THT (tetrahydrothiophene) ligand. As anticipated, the palladium complex **2** substituted the THT ligand and the only product formed, [Pd(dmab)-(κ<sup>2</sup>-P,O-PPh<sub>2</sub>NC(O)Me)AuCl] (**6**), was isolated in good yield. This new complex is stable for a few days when kept in CDCl<sub>3</sub> at room temperature under exclusion of light; it neither decomposes nor rearranges. The solid-state structure determination by X-ray diffraction (Figure 3a, Table 1) established the formation of a Au–N bond. Its length of 2.035(4) Å is slightly shorter than in the related cationic complex [Au(PPh<sub>3</sub>)(**2**)]OTf (2.085(6) Å).<sup>1</sup> Formally, complex **2** has behaved as a neutral, 2e donor ligand (L-type) toward the Au(I) center which retains its usual 14e electronic configuration. Bond distances in this heterodimetallic complex are further discussed below. In the solid state, the molecules are arranged in centrosymmetrical pairs (Figure 3b), which leads to a better packing and to an intermolecular Au–Au separation of 3.88(1) Å, which may provide additional stabilization, although typical d<sup>10</sup>–d<sup>10</sup> aurophilic interactions generally correspond to Au–Au distances of 3.00 ± 0.25 Å.<sup>7</sup>

When [Au(THT)<sub>2</sub>]OTf, prepared in situ, was used as a precursor with the hope that a Au/Pd coordination polymer could form by analogy with **3**·OTf, the complex [Pd(dmab)(κ<sup>2</sup>-P,O-PPh<sub>2</sub>NC(O)Me)Au(THT)]OTf (**7**·OTf) was obtained instead (Scheme 2). It was purified by recrystallization, although it shows only limited stability in solution and at room temperature. The following alternative procedures yielded **7**·X (X = OTf, BF<sub>4</sub>) but with larger amounts of byproducts: (i) addition of a CH<sub>2</sub>Cl<sub>2</sub> solution of [Au(THT)]BF<sub>4</sub> to **2** in CH<sub>2</sub>Cl<sub>2</sub>, (ii) addition of the coordination polymer [Ag(**2**)]OTf<sub>n</sub> in THF to a solution of [AuCl(THT)] in THF, and (iii) mixing of **6**, AgOTf, and THT in CH<sub>2</sub>Cl<sub>2</sub>. The most abundant byproduct, [Pd(dmab)(κ<sup>2</sup>-P,O-PPh<sub>2</sub>NC(O)Me)]<sub>2</sub>AuX (**8**·X) (Scheme 3), resulted from a double

(4) Andrieu, J.; Braunstein, P.; Drillon, M.; Dusausoy, Y.; Ingold, F.; Rabu, P.; Tiripicchio, A.; Uguzzoli, F. *Inorg. Chem.* **1996**, *35*, 5986.

(5) Veya, P.; Floriani, C.; Chiesi-Villa, A.; Guastini, C.; Dedieu, A.; Ingold, F.; Braunstein, P. *Organometallics* **1993**, *12*, 4359.

(6) Apfelbacher, A.; Braunstein, P.; Brissieux, L.; Welter, R. *Dalton Trans.* **2003**, 1669, and references therein.

(7) Pyykkö, P. *Angew. Chem., Int. Ed.* **2004**, *43*, 4412, and references therein.

(8) Ahrens, B.; Jones, P. G. Z. *Naturforsch., B: Chem. Sci.* **2000**, *55*, 803.

(9) Vicente, J.; Chicote, M. T.; Guerrero, R.; Ramirez de Arellano, M. C. *Chem. Commun.* **1999**, 1541.

(10) Lock, C. J. L.; Wang, Z. *Acta Crystallogr., Sect. C: Cryst. Struct. Commun.* **1993**, *49*, 1330.



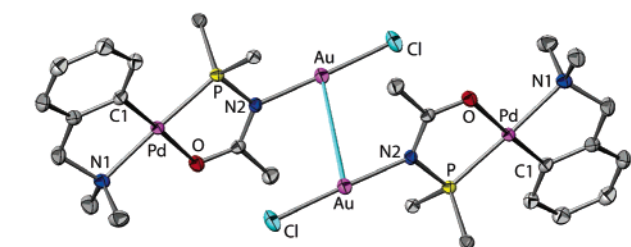
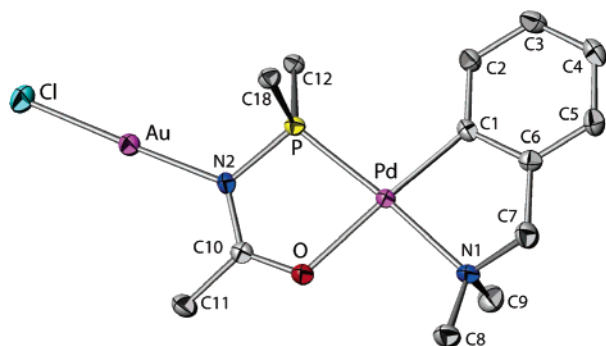
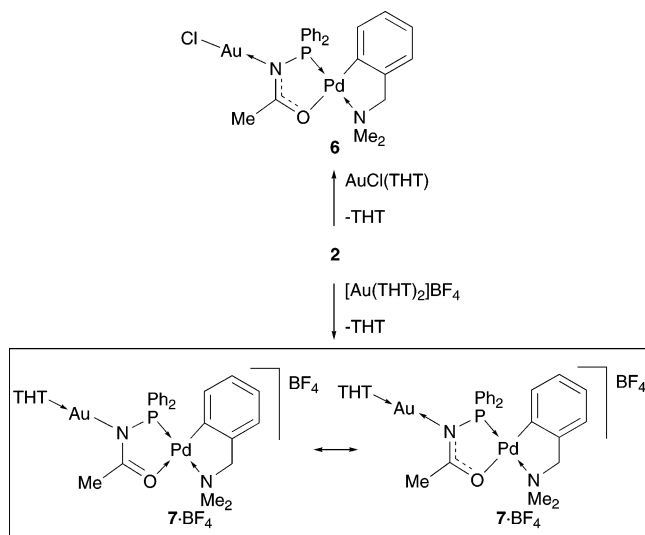


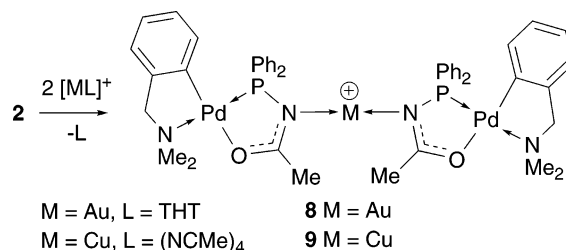
**Figure 3.** (a) ORTEP view of the structure of  $[\{Pd(dmmba)(\kappa^2\text{-}P,O\text{-}PPh_2NC(O)Me)\}AuCl]$  (**6**) with the atom-numbering scheme. Only the *ipso* aryl carbon atoms on P are shown for clarity. Thermal ellipsoids enclose 50% of the electron density. Selected bond distances (Å) and angles (deg): Au–N(2) 2.035(4), Au–Cl 2.256(2), Pd–C(1) 2.001(5), Pd–O 2.118(4), Pd–N(1) 2.124(4), Pd–P 2.204(1), P–N(2) 1.701(4), N(2)–C(10) 1.347(6), C(10)–C(11) 1.497(7), C(10)–O 1.265(6); N(2)–Au–Cl 178.3(1), C(1)–Pd–O 176.9(2), C(1)–Pd–N(1) 82.8(2), O–Pd–N(1) 95.1(2), C(1)–Pd–P 101.2(2), O–Pd–P 81.0(1), N(1)–Pd–P 176.1(1), P–Pd–N(2) 102.5(2), Au–N(2)–C(10) 124.8(3), P–N(2)–Au 119.8(2), P–N(2)–C(10) 115.4(3), N(2)–C(10)–C(11) 118.3(4), N(2)–C(10)–O 123.1(5), C(11)–C(10)–O 118.6(4), C(10)–O–Pd 116.8(3). (b) ORTEP view of the pairwise arrangement of the molecules of  $[\{Pd(dmmba)(\kappa^2\text{-}P,O\text{-}PPh_2NC(O)Me)\}AuCl]$  (**6**) in the solid state. Au–Au = 3.88(1) Å.

### Scheme 2. Behavior of **2** as an L- or X-Type Metalloligand



substitution at the gold center by **2**, and its direct synthesis will be discussed below. Another byproduct often observed was  $5^+$ , whose direct formation from **2** is explained by the presence of traces of acid in the

### Scheme 3. Synthesis of Trinuclear Pd/M/Pd Complexes



reaction mixture. The reduced stability of **7**·OTf compared to that of  $[Au(PPh_3)(\mathbf{2})]OTf^1$  probably results from the presence of the weaker and more loosely bound THT ligand compared to  $PPh_3$ . However, the fact that the THT donor remained coordinated to Au prevented the formation of a coordination polymer analogous to that characterized in the Pd–Ag system **3**·OTf.<sup>1</sup> The molecular structure of **7**·BF<sub>4</sub> was determined by single-crystal X-ray diffraction. Its Au–N and Au–S bond lengths, 2.052(6) and 2.253(3) Å, respectively, are very similar to those in a related Au(THT) complex, where a dimethylamido ligand is bonded to Au (av Au–N distance: 2.06 Å, av Au–S distance: 2.26 Å).<sup>8</sup> The metalloligand **2** behaves formally as an X-type ligand in **7**<sup>+</sup>, and the length of the Au–N bond is intermediate between those in **6** and in  $[Au(PPh_3)(\mathbf{2})]OTf$ , where the N–Au interaction is formally dative and covalent, respectively. We come back to this point below.

Compound **8**·BF<sub>4</sub>, which was one of the byproducts formed during the synthesis of **7**·BF<sub>4</sub>, was obtained directly from  $[Au(THT)]BF_4$  and 2 equiv of **2** by analogy with the synthesis of  $[Ag(\mathbf{2})_2]OTf$ .<sup>1</sup> The X-ray structure analysis revealed nearly identical bond distances within the two Pd moieties (Figure 5, Table 1). The molecular

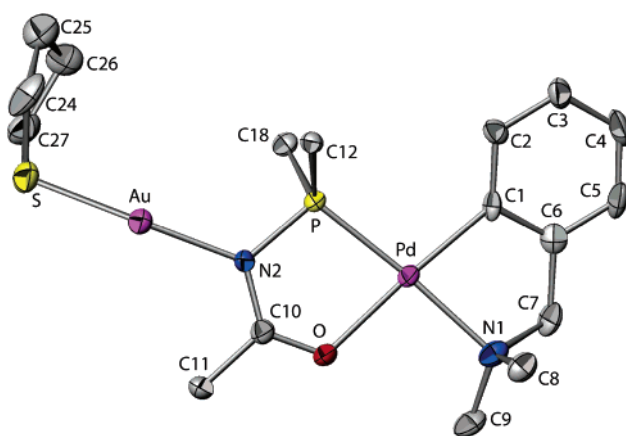


**Figure 4.** ORTEP view of the structure of  $[\{Pd(dmmba)(\kappa^2\text{-}P,O\text{-}PPh_2NC(O)Me)\}Au(THT)]^+$  in **7**·BF<sub>4</sub> with the atom-numbering scheme. Only the *ipso* aryl carbon atoms on P are shown for clarity. Thermal ellipsoids enclose 50% of the electron density. Selected bond distances (Å) and angles (deg): Au–N(2) 2.052(6), Au–S 2.253(3), S–C(24) 1.77(1), S–C(27) 1.83(1), Pd–C(1) 2.011(8), Pd–O 2.108(5), Pd–N(1) 2.120(7), Pd–P 2.211(2), P–N(2) 1.704(6), N(2)–C(10) 1.342(9), C(10)–O 1.236(9); N(2)–Au–S 174.5(2), C(1)–Pd–O 176.7(3), C(1)–Pd–N(1) 82.4(3), O–Pd–N(1) 94.3(2), C(1)–Pd–P 101.5(2), O–Pd–P 81.8(2), N(1)–Pd–P 175.7(2), Pd–P–N(2) 101.4(2), P–N(2)–Au 119.0(3), Au–N(2)–C(10) 125.4(5), N(2)–C(10)–C(11) 117.4(7), N(2)–C(10)–O 125.0(7), C(10)–O–Pd 116.4(5).

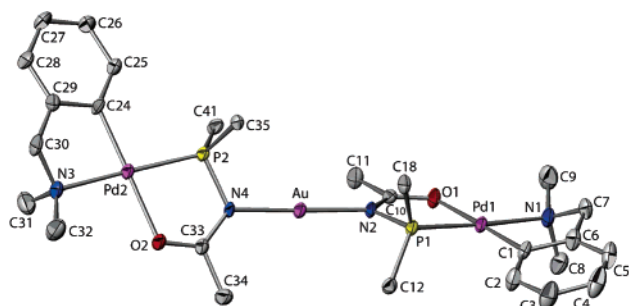


**Figure 5.** ORTEP view of the structure of  $[\{\text{Pd}(\text{dmmba})-(\kappa^2\text{-}P,O\text{-PPh}_2\text{NC}(\text{O})\text{Me})\}\text{Au}]^+$  in  $\mathbf{8}\cdot\text{BF}_4\cdot 2\text{CH}_2\text{Cl}_2$  with the atom-numbering scheme. Only the *ipso* aryl carbon atoms on P are shown for clarity. Thermal ellipsoids enclose 50% of the electron density. Selected bond distances (Å) and angles (deg): Au–N(2) 2.033(4), Au–N(4) 2.034(4), Pd(1)–C(1) 1.995(6), Pd(1)–O(1) 2.136(4), Pd(1)–N(1) 2.138(5), Pd(1)–P(1) 2.204(2), P(1)–N(2) 1.708(5), N(2)–C(10) 1.344(7), C(10)–O(1) 1.250(6), Pd(2)–C(24) 1.995(5), Pd(2)–N(3) 2.131(5), Pd(2)–O(2) 2.134(4), Pd(2)–P(2) 2.206(2), P(2)–N(4) 1.709(5), N(4)–C(33) 1.328(7), C(33)–O(2) 1.255(6); N(2)–Au–N(4) 178.2(2), C(1)–Pd(1)–O(1) 178.7(2), C(1)–Pd(1)–N(1) 82.1(2), O(1)–Pd(1)–N(1) 98.1(2), C(1)–Pd(1)–P(1) 98.8(2), O(1)–Pd(1)–P(1) 81.1(1), N(1)–Pd(1)–P(1) 177.0(2), Pd(1)–P(1)–N(2) 102.7(2), P(1)–N(2)–Au 116.5(2), Au–N(2)–C(10) 128.2(4), N(2)–C(10)–C(11) 117.5(5), N(2)–C(10)–O(1) 124.1(5), C(10)–O(1)–Pd(1) 116.8(4), C(24)–Pd(2)–O(2) 177.7(2), C(24)–Pd(2)–N(3) 82.2(2), O(2)–Pd(2)–N(3) 98.2(2), C(24)–Pd(2)–P(2) 99.3(2), O(2)–Pd(2)–P(2) 80.5(1), N(3)–Pd(2)–P(2) 176.8(2), Pd(2)–P(2)–N(4) 102.6(2), P(2)–N(4)–Au 115.8(2), Au–N(4)–C(33) 128.5(4), N(4)–C(33)–C(34) 117.6(5), N(4)–C(33)–O(2) 123.4(5), C(33)–O(2)–Pd(2) 117.2(4).

structure of  $\mathbf{8}\cdot\text{BF}_4$  and in particular the Au–N bond lengths of 2.033(4) and 2.034(4) Å are comparable with those of complexes in which a gold center is coordinated, for example, by two pyrimidine moieties (av Au–N distance: 2.04 Å)<sup>9</sup> or two imidazole moieties (av Au–N distance: 2.01 Å).<sup>10</sup>

Although attempts to isolate Pd/Tl complexes from the reactions between **2** and TlPF<sub>6</sub> or between **5**·OTf and TlOEt or TlOAc failed, Cu(I) could be used to form a linear complex with two metalloligands **2** and the trinuclear Pd/Cu/Pd complex  $[\{\text{Pd}(\text{dmmba})(\kappa^2\text{-}P,O\text{-PPh}_2\text{NC}(\text{O})\text{Me})\}_2\text{Cu}]\text{BF}_4$  (**9**·BF<sub>4</sub>) was obtained in good yield from the reaction between  $[\text{Cu}(\text{NCMe})_4]\text{BF}_4$  and 2 equiv of **2**. The reaction between  $[\text{Cu}(\text{NCMe})_4]\text{BF}_4$  and only 1 equiv of **2** led to three products: the reprotonated form **5**·BF<sub>4</sub>, the bis-substituted complex **9**·BF<sub>4</sub>, and a third product (**10**·BF<sub>4</sub>) with probably a 1:1 Pd/Cu stoichiometry were detected in the <sup>31</sup>P{<sup>1</sup>H} NMR spectrum, but further purification remained unsuccessful and only **5**·BF<sub>4</sub><sup>3</sup> was crystallized. An X-ray analysis was performed on single crystals of **9**·BF<sub>4</sub> and showed a structure related to those of  $[\text{Ag}(\mathbf{2})_2]\text{OTf}^1$  and of the analogous Au complex **8**·BF<sub>4</sub> (Figure 6, Tables 1). The two Pd moieties in **9**·BF<sub>4</sub> have again similar bond distances and the two Cu–N bond lengths are almost identical at 1.873(3) and 1.877(4) Å. This structure is further discussed below.

A comparison of the main bond distances in complexes **6**, **7**·BF<sub>4</sub>, and  $[\text{Au}(\text{PPh}_3)(\mathbf{2})]\text{OTf}^1$  and **8**·BF<sub>4</sub> is provided in Table 1. Whereas the data for **7**<sup>+</sup> indicate, as expected, a bonding scheme similar to that in **5**<sup>+</sup>, the structural and spectroscopic similarities between **6** and

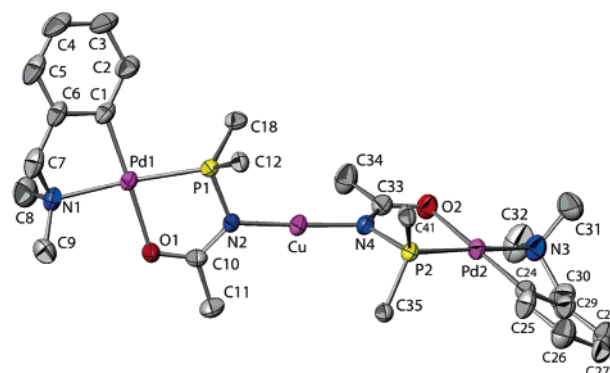


**Figure 6.** ORTEP view of the structure of  $[\{\text{Pd}(\text{dmmba})-(\kappa^2\text{-}P,O\text{-PPh}_2\text{NC}(\text{O})\text{Me})\}_2\text{Cu}]^+$  in  $\mathbf{9}\cdot\text{BF}_4$  with the atom-numbering scheme. Only the *ipso* aryl carbon atoms on P are shown for clarity. Thermal ellipsoids enclose 50% of the electron density. Selected bond distances (Å) and angles (deg): Cu–N(2) 1.873(3), Cu–N(4) 1.877(4), Pd(1)–C(1) 1.993(5), Pd(1)–O(1) 2.124(3), Pd(1)–N(1) 2.130(4), Pd(1)–P(1) 2.203(2), P(1)–N(2) 1.712(4), N(2)–C(10) 1.333(6), C(10)–O(1) 1.261(5), Pd(2)–C(24) 1.997(5), Pd(2)–O(2) 2.113(3), Pd(2)–N(3) 2.134(4), Pd(2)–P(2) 2.218(1), P(2)–N(4) 1.716(4), N(4)–C(33) 1.336(6), C(33)–O(2) 1.264(5); N(2)–Cu–N(4) 178.0(2), C(1)–Pd(1)–O(1) 176.1(2), C(1)–Pd(1)–N(1) 82.8(2), O(1)–Pd(1)–N(1) 95.8(1), C(1)–Pd(1)–P(1) 100.7(2), O(1)–Pd(1)–P(1) 80.98(9), N(1)–Pd(1)–P(1) 173.7(1), Pd(1)–P(1)–N(2) 103.0(1), P(1)–N(2)–Cu 117.4(2), Cu–N(2)–C(10) 128.0(3), N(2)–C(10)–C(11) 118.4(4), N(2)–C(10)–O(1) 124.8(4), C(10)–O(1)–Pd(1) 116.5(3), C(24)–Pd(2)–O(2) 176.9(2), C(24)–Pd(2)–N(3) 82.3(2), O(2)–Pd(2)–N(3) 94.9(2), C(24)–Pd(2)–P(2) 101.8(2), O(2)–Pd(2)–P(2) 80.9(1), N(3)–Pd(2)–P(2) 174.0(1), Pd(2)–P(2)–N(4) 102.1(1), P(2)–N(4)–Cu 120.5(2), Cu–N(4)–C(33) 124.3(3), N(4)–C(33)–C(34) 118.9(4), N(4)–C(33)–O(2) 123.6(4), C(33)–O(2)–Pd(2) 117.4(3).

**7**·BF<sub>4</sub> are rather surprising since in the former case the metalloligand **2** behaves as a neutral, 2e donor ligand, in contrast to the latter case, where a more covalent Au–N bonding was expected. This could indicate that in the latter complex a mesomeric structure in which the positive charge of the complex is formally more localized on the Au(I) center represents a strong contribution to the bonding (Scheme 2). One could have expected the Au–N bond lengths in complexes **6**, **7**·BF<sub>4</sub>, and **8**·BF<sub>4</sub> to reflect the bonding situation within the Pd fragment, whether it behaves more like an L-type (**A**) or X-type (**B**) metalloligand. But surprisingly, there are no significant differences between the Au–N distances, of 2.035(4) Å in **6**, 2.052(6) Å in **7**·BF<sub>4</sub>, and 2.033(4)/2.034(4) Å, in **8**·BF<sub>4</sub>. The linear geometry around the gold center is retained throughout the series **6** (Cl–Au–N(2) = 178.3(1)°), **7**·BF<sub>4</sub> (S–Au–N(2) = 174.5(2)°), and **8**·BF<sub>4</sub> (N(2)–Au–N(4) = 178.2(2)°). The π-system within the phosphino iminolate appears to be rather localized for these three compounds, with a more pronounced double-bond character for the C=O than for the C–N bond: the C=O bond lengths of 1.265(6) Å in **6**, 1.236(9) Å in **7**·BF<sub>4</sub>, and 1.250(6)/1.255(6) Å in **8**·BF<sub>4</sub> are similar to that in complex **5**·OTf (1.251(3) Å), and all C–N bond lengths are nearly identical within the standard deviation (1.347(3) Å in **5**·OTf, 1.347(6) Å in **6**, 1.342(9) Å in **7**·BF<sub>4</sub>, and 1.344(7)/1.328(7) Å in **8**·BF<sub>4</sub>). These values compare very well with those in **9**·BF<sub>4</sub>,

which has C=O distances of 1.261(5)/1.264(5) Å and C–N distances of 1.333(6)/1.336(6) Å (Scheme 3, Table 1).

The only significant structural difference between the three analogous compounds  $[M(\mathbf{2})_2]^+$ , where M is Cu, Ag, or Au, was found in the dihedral angle formed by the two Pd,P,N,C,O planes: 79(1)° (M = Cu), 67(1)° (M = Ag),<sup>1</sup> and 61(1)° (M = Au). These differences are due to packing effects since rotations of small amplitude of the molecular fragments about the N–M–N axis should be facile both electronically ( $\sigma$ -bond) and sterically. The average M–N bond distances of 1.875(4) Å for M = Cu, 2.118(5) Å for M = Ag, and 2.033(4) Å for M = Au follow the same trend as the sums of the covalent radii for N in a single bond (0.70 Å)<sup>11</sup> and the two-coordinated metals:<sup>12</sup> 1.13 + 0.70 = 1.83 Å for Cu–N, 1.33 + 0.70 = 2.03 Å for Ag–N, and 1.25 + 0.70 = 1.95 Å for Au–N, respectively. The coordination number of 2 in complexes  $\mathbf{8}\cdot\text{BF}_4$  and  $\mathbf{9}\cdot\text{BF}_4$  is not unusual for Au<sup>I</sup>, which appears in ca. 80% of its complexes in a linear coordination geometry, whereas Cu<sup>I</sup> is found in only ca. 10% with this coordination number.<sup>13</sup> For comparison, less than 25% of the silver complexes have the metal in a coordination number of 2.<sup>13</sup> Although the coordination geometry around the metal center in  $[\text{Ag}(\mathbf{2})_2]\text{OTf}$  is almost linear (N(2)–Ag–N(4) = 175.4(2)°), a weak electrostatic interaction between a triflate oxygen and Ag<sup>+</sup> of 2.82(1) Å was noted.<sup>1</sup>

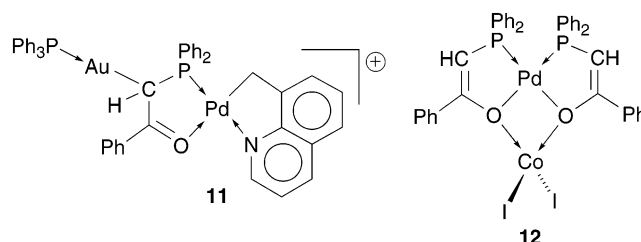
A comparison between the  $\nu(\text{NC}+\text{CO})$  vibration frequencies of  $\mathbf{2}$  and  $\mathbf{5}\cdot\text{OTf}$  with those of the complexes in which  $\mathbf{2}$  behaves as a metalloligand (measured in KBr for a better resolution, Table 1) reveals no obvious correlation with the N(2)–C, C–O, and N(2)–M bond orders. Similar observations have been made previously in the case of related phosphino-enolate complexes.<sup>14</sup> Here we observe that the  $\nu(\text{NC}+\text{CO})$  vibration frequencies are similar in our complexes and comparable to that of the precursor  $\mathbf{2}$ . None of the heterometallic complexes show a  $\nu(\text{NC}+\text{CO})$  frequency similar to that of compound  $\mathbf{5}\cdot\text{OTf}$ .

Considering the isolobal relationship between H<sup>+</sup> and  $[\text{Au}(\text{L})]^+$ , we wondered whether formation of a homodinuclear complex of the type  $[\{\text{Pd}(\text{dmba})(\kappa^2\text{-P},\text{O}-\text{PPh}_2\text{NC}(\text{O})\text{Me})\}_2\text{H}]\text{OTf}$  with a central N–H–N unit would be possible since a molecule of  $\mathbf{2}$  could behave as a base toward a molecule of  $\mathbf{5}\cdot\text{OTf}$ . When mixing equimolar amounts of compounds  $\mathbf{2}$  and  $\mathbf{5}\cdot\text{OTf}$ , the  $^{31}\text{P}\{^1\text{H}\}$  NMR spectrum in  $\text{CD}_2\text{Cl}_2$  showed only one signal at a chemical shift value average between those of the two reagents. Upon crystallization from a  $\text{CH}_2\text{Cl}_2$  or THF solution layered with pentane, only the more polar  $\mathbf{5}\cdot\text{OTf}$  began to crystallize. This result contrasts with the behavior of related compounds where a proton was trapped, for example, between two pyridine or imidazole moieties.<sup>15</sup> Changing the counterion to  $\text{PF}_6^-$  and using more polar solvents such as THF or a THF/MeCN mixture did not lead to the isolation of the desired

product. Low-temperature  $^{31}\text{P}\{^1\text{H}\}$  NMR studies showed that at 181 K the signal was split into two signals corresponding to  $\mathbf{2}$  and  $\mathbf{5}\cdot\text{OTf}$ . The occurrence of a dynamic equilibrium between these precursors and the desired adduct is further supported by the observation that when the reaction mixture was enriched with one of the two precursors, the  $^{31}\text{P}\{^1\text{H}\}$  NMR signal shifted toward its chemical shift value.

## Conclusion

We have shown in this work that the palladium phosphino-iminolate complex  $\mathbf{2}$  readily behaves as an elementary building block toward electrophilic coinage metal complexes to form heterodi- or trinuclear complexes. This occurs by selective coordination of the metal to the  $\text{sp}^2$ -hybridized nitrogen atom of the P,O chelate. The nature of the resulting metal–nitrogen bond can be interpreted according to two limiting forms, represented by **A** and **B**, respectively. Although the structural parameters clearly reflect the higher electronic delocalization within the N–C–O moiety of  $\mathbf{2}$  compared to  $\mathbf{5}^+$ , in which the C=O bond order is higher, no significant differences were observed in the heterometallic complexes between the P–N, N–C, or C–O bond distances within the metalloligand as a function of its behavior as a formal L- or X-type ligand. This emphasizes the bonding versatility of this synthon. Related studies with phosphino-enolate complexes have shown that soft metal centers bind to their carbon, as in **11**, whereas harder ions can coordinate to the oxygen donors of the P,O chelates, as in **12**.<sup>4</sup>



In these cases, the dichotomy encountered in the present work did not apply since the carbon–metal bond was formally only of a covalent type.

## Experimental Section

**General Procedures.** All manipulations were carried out under inert dinitrogen atmosphere, using standard Schlenk-line conditions and dried and freshly distilled solvents. The  $^1\text{H}$ ,  $^{31}\text{P}\{^1\text{H}\}$ ,  $^{13}\text{C}\{^1\text{H}\}$ ,  $^{19}\text{F}\{^1\text{H}\}$ , and  $^{31}\text{P}\{^1\text{H}\}$  NMR spectra were recorded unless otherwise stated on a Bruker Avance 300 instrument at 300.13, 75.47, 282.40, and 121.49 MHz, respectively, using TMS,  $\text{CFCl}_3$ , or  $\text{H}_3\text{PO}_4$  (85% in  $\text{D}_2\text{O}$ ) as external standards with downfield shifts reported as positive. All NMR spectra were measured at 298 K, unless otherwise specified. The assignment of the signals was made by  $^1\text{H}$ ,  $^1\text{H}$ -COSY and  $^1\text{H}$ ,  $^{13}\text{C}$ -HMQC experiments. IR spectra in the range 4000–400  $\text{cm}^{-1}$  were recorded as KBr pellets on a FT-IR IFS66 Bruker spectrometer. Elemental C, H, and N analyses were performed by the “Service de Microanalyses”, Université Louis Pasteur, Strasbourg.

(11) Holleman, A. F.; Wiberg, E. *Lehrbuch der Anorganischen Chemie*, 91–100. ed.; de Gruyter: Berlin, 1985; p 133.

(12) Tripathi, U. M.; Bauer, A.; Schmidbaur, H. *J. Chem. Soc., Dalton Trans.* **1997**, 2865.

(13) Carvajal, M. A.; Novoa, J. J.; Alvarez, S. *J. Am. Chem. Soc.* **2004**, *126*, 1465.

(14) Veya, P.; Floriani, C.; Chiesi-Villa, A.; Guastini, C.; Dedieu, A.; Ingold, F.; Braunstein, P. *Organometallics* **1993**, *12*, 4359.

(15) See for example: (a) Glidewell, C.; Holden, H. D. *Acta Crystallogr., Sect. B: Struct. Crystallogr. Cryst. Chem.* **1982**, *38*, 667. (b) Potrzebowski, M. J.; Cypryk, M.; Michalska, M.; Kozioł, A. E.; Kazmierski, S.; Ciesielski, W.; Klinowski, J. *Phys. Chem. B* **1998**, *102*, 4488. (c) Mautner, F. A.; Goher, M. S. A.; Grech. *Polyhedron* **1999**, *18*, 553.



When  $\text{BF}_4^-$  was used as a counterion, the  $^{19}\text{F}\{^1\text{H}\}$  spectra provided the appropriate signal with the pattern typical for  $\text{B}^{10}\text{-F}^{19}$  and  $\text{B}^{11}\text{-F}^{19}$  shifts.<sup>16</sup> The following compounds were synthesized according to literature procedures or improved syntheses:  $[\text{Pd}(\text{dmba})(\kappa^2\text{-P,O-PPh}_2\text{NC(O)Me})]$  (**2**),<sup>1</sup>  $[\text{Pd}(\text{dmba})(\kappa^2\text{-P,O-PPh}_2\text{NHC(O)Me})\text{OTf}]$  (**5-OTf**),<sup>2</sup>  $[\text{AuCl}(\text{THT})]$ ,<sup>17</sup>  $[\text{Cu}(\text{NCMe})_4]\text{BF}_4$ .<sup>18</sup> Other chemicals were commercially available and used as received. All yields given are based on Pd unless otherwise stated.

**Preparation of  $[\text{Pd}(\text{dmba})(\kappa^2\text{-P,O-PPh}_2\text{N}\text{---}(\text{---O)Me})]$  (**2**). Improved Synthesis.** The product can be directly synthesized in a one-pot reaction from 0.5 equiv of  $[\text{Pd}(\text{dmba})(\mu\text{-Cl})_2]$ , 1 equiv of  $\text{PPh}_2\text{NHC(O)Me}$ , and 1 equiv of  $\text{KO}t\text{-Bu}$  in THF and stirring overnight. After removing the solvent in vacuo and extraction of the residue with  $\text{CH}_2\text{Cl}_2$ , purification can be done as published to receive the product in  $\geq 80\%$  yield.  $^1\text{H}$  NMR ( $\text{CDCl}_3$ ):  $\delta$  2.22 (d, 3H,  $^4J_{\text{P-H}} = 0.9$  Hz,  $\text{C(O)CH}_3$ ), 2.85 (d, 6H,  $^4J_{\text{P-H}} = 2.1$  Hz,  $\text{N(CH}_3)_2$ ), 3.92 (d, 2H,  $^4J_{\text{P-H}} = 1.7$  Hz,  $\text{NCH}_2$ ), 6.65–6.70 (m, 1H, aryl-CH, dmba), 6.80–6.95 (m, 2H, aryl-CH, dmba), 7.00–7.05 (m, 1H, aryl-CH, dmba), 7.35–7.50 (m, 6H, *m*-, *p*-aryl,  $\text{PPh}_2$ ), 7.70–7.80 (m, 4H, *o*-aryl,  $\text{PPh}_2$ ).  $^{31}\text{P}\{^1\text{H}\}$  NMR ( $\text{CDCl}_3$ ):  $\delta$  81.9 (s,  $\text{PPh}_2$ ).

**Preparation of  $[\text{Pd}(\text{dmba})(\kappa^2\text{-P,O-PPh}_2\text{NHC(O)Me})\text{OTf}]$  (**5-OTf**). Improved Synthesis.** The product can also be directly synthesized in a one-pot reaction from 1 equiv of  $\text{PPh}_2\text{NHC(O)Me}$ , 0.5 equiv of  $[\text{Pd}(\text{dmba})(\mu\text{-Cl})_2]$ , and 1 equiv of  $\text{AgOTf}$  in  $\text{CH}_2\text{Cl}_2$ . The workup was done as described and the product isolated in  $\geq 80\%$  yield.<sup>2</sup>

$[\text{Pd}(\text{dmba})(\kappa^2\text{-P,O-PPh}_2\text{NHC(O)Me})\text{PF}_6]$  (**5-PF<sub>6</sub>**) can be prepared analogously by the use of  $\text{TIPF}_6$  instead of  $\text{AgOTf}$ .  $^1\text{H}$  NMR ( $\text{CDCl}_3$ ):  $\delta$  2.44 (d, 3H,  $^4J_{\text{P-H}} = 0.6$  Hz,  $\text{C(O)CH}_3$ ), 2.93 (d, 6H,  $^4J_{\text{P-H}} = 3.0$  Hz,  $\text{N(CH}_3)_2$ ), 4.07 (d, 2H,  $^4J_{\text{P-H}} = 2.4$  Hz,  $\text{NCH}_2$ ), 6.60–6.65 (m, 1H, aryl-CH, dmba), 6.75–6.80 (m, 1H, aryl-CH, dmba), 7.00–7.10 (m, 2H, aryl-CH, dmba), 7.50–7.65 (m, 6H, *m*-, *p*-aryl,  $\text{PPh}_2$ ), 7.80–7.90 (m, 4H, *o*-aryl,  $\text{PPh}_2$ ), 10.75 (br s, 1H, NH).  $^{19}\text{F}\{^1\text{H}\}$  NMR ( $\text{CDCl}_3$ ):  $\delta$  -78.8 (s, OTf).  $^{31}\text{P}\{^1\text{H}\}$  NMR ( $\text{CDCl}_3$ ):  $\delta$  80.4 (s,  $\text{PPh}_2$ ).

**Preparation and Spectroscopic Data for  $[\{\text{Pd}(\text{dmba})(\kappa^2\text{-P,O-PPh}_2\text{NC(O)Me})\}\text{AuCl}]$  (**6**).** Solid  $[\text{AuCl}(\text{THT})]$  (0.20 g, 0.62 mmol) was suspended in toluene (15 mL), and  $\text{CH}_2\text{Cl}_2$  (ca. 1 mL) was added to ensure dissolution. Solid **2** (0.30 g, 0.62 mmol) was dissolved in toluene (20 mL) and added slowly to the solution of  $[\text{AuCl}(\text{THT})]$ . A colorless precipitate was formed after 5 min, and the mixture was stirred for 15 min. After filtration, the residue was washed with toluene (5 mL) and dried in vacuo (0.33 g, 0.46 mmol, 74%). Single crystals suitable for X-ray diffraction were obtained by layering a  $\text{CDCl}_3$  solution with pentane.  $^1\text{H}$  NMR ( $\text{CDCl}_3$ ):  $\delta$  2.48 (d, 3H,  $^4J_{\text{P-H}} = 0.5$  Hz,  $\text{C(O)CH}_3$ ), 2.86 (d, 6H,  $^4J_{\text{P-H}} = 2.6$  Hz,  $\text{N(CH}_3)_2$ ), 3.96 (d, 2H,  $^4J_{\text{P-H}} = 1.7$  Hz,  $\text{NCH}_2$ ), 6.65–6.75 (m, 2H, aryl-CH, dmba), 6.90–7.05 (m, 2H, aryl-CH, dmba), 7.40–7.60 (m, 6H, *m*-, *p*-aryl,  $\text{PPh}_2$ ), 7.90–8.10 (m, 4H, *o*-aryl,  $\text{PPh}_2$ ).  $^{13}\text{C}\{^1\text{H}\}$  NMR ( $\text{CDCl}_3$ ):  $\delta$  26.1 (d,  $^3J_{\text{P-C}} = 8.2$  Hz,  $\text{C(O)CH}_3$ ), 50.0 (d,  $^3J_{\text{P-C}} = 2.7$  Hz,  $\text{N(CH}_3)_2$ ), 70.8 (d,  $^{3+4}J_{\text{P-C}} = 3.3$  Hz,  $\text{NCH}_2$ ), 123.0 (s, aryl, dmba), 124.9 (s, aryl, dmba), 126.3 (d,  $J_{\text{P-C}} = 4.9$  Hz, aryl, dmba), 129.0 (d,  $^3J_{\text{P-C}} = 11.8$  Hz, *m*-aryls,  $\text{PPh}_2$ ), 130.9 (d,  $^1J_{\text{P-C}} = 59.6$  Hz, *ipso*-aryls,  $\text{PPh}_2$ ), 132.3 (d,  $^4J_{\text{P-C}} = 2.9$  Hz, *p*-aryls,  $\text{PPh}_2$ ), 133.8 (d,  $^2J_{\text{P-C}} = 14.3$  Hz, *o*-aryls,  $\text{PPh}_2$ ), 138.1 (d,  $J_{\text{P-C}} = 9.9$  Hz, aryl, dmba), 146.0 (s,  $\text{C}_q\text{-dmba}$ ), 148.9 (d,  $J_{\text{P-C}} = 1.9$  Hz,  $\text{C}_q\text{-dmba}$ ), 187.9 (d,  $^{2+3}J_{\text{P-C}} = 3.9$  Hz, CO).  $^{31}\text{P}\{^1\text{H}\}$  NMR ( $\text{CDCl}_3$ ):  $\delta$  94.1 (s,  $\text{PPh}_2$ ).  $^{31}\text{P}\{^1\text{H}\}$  NMR ( $\text{CD}_2\text{Cl}_2$ ):  $\delta$  93.9 (s,  $\text{PPh}_2$ ). IR (KBr, select.):  $\nu(\text{NC+CO})$  1506  $\text{cm}^{-1}$ . Anal. Calcd for  $\text{C}_{23}\text{H}_{25}\text{AuClIN}_2\text{OPd}$  (715.27): C, 38.62; H, 3.52; N, 3.92. Found: C, 38.95; H, 3.74; N, 3.53.

**Preparation and Spectroscopic Data for  $[\{\text{Pd}(\text{dmba})(\kappa^2\text{-P,O-PPh}_2\text{NC(O)Me})\}\text{Au}(\text{tth})\text{OTf}]$  (**7-OTf**). Method A.**

To a solution of  $[\text{AuCl}(\text{THT})]$  (0.10 g, 0.31 mmol) in  $\text{CH}_2\text{Cl}_2$  (20 mL) were added THT (2 mL) and solid  $\text{AgOTf}$  (0.08 g, 0.31 mmol). An off-white precipitate was formed immediately, and the mixture was stirred for 1 h at room temperature. After filtration via cannula the solvent was removed in vacuo to yield  $[\text{Au}(\text{THT})_2]\text{OTf}$  as a yellow powder (0.13 g, 0.25 mmol, 81% based on Au). The residue was redissolved in  $\text{CH}_2\text{Cl}_2$  (10 mL), and a  $\text{CH}_2\text{Cl}_2$  (10 mL) solution of **2** (0.11 g, 0.25 mmol) was added. The mixture was stirred for 1 h, and the solvent was removed in vacuo. The composition of the residue was controlled by  $^{31}\text{P}\{^1\text{H}\}$  NMR spectroscopy, and the three phosphorus-containing fragments **5<sup>+</sup>**, **7<sup>+</sup>** and **8<sup>+</sup>** were found in a ratio 1:15:4, respectively.  $^{31}\text{P}\{^1\text{H}\}$  NMR ( $\text{CD}_2\text{Cl}_2$ ):  $\delta$  79.7 (s,  $\text{PPh}_2$  in **5<sup>+</sup>**), 92.7 (s,  $\text{PPh}_2$  in **7<sup>+</sup>**), 94.0 (s,  $\text{PPh}_2$  in **8<sup>+</sup>**).

Purification was achieved by recrystallization from a  $\text{CH}_2\text{Cl}_2$  solution layered with pentane at 5 °C overnight (0.14 g, 0.15 mmol, 60%).  $^1\text{H}$  NMR ( $\text{CD}_2\text{Cl}_2$ ):  $\delta$  2.06 (br s, 4H,  $\text{CH}_2$ , THT), 2.45 (d, 3H,  $^4J_{\text{P-H}} = 1.0$  Hz,  $\text{C(O)CH}_3$ ), 2.88 (d, 6H,  $^4J_{\text{P-H}} = 2.7$  Hz,  $\text{N(CH}_3)_2$ ), 3.44 (br s, 4H,  $\text{SCH}_2$ , THT), 4.00 (d, 2H,  $^4J_{\text{P-H}} = 2.1$  Hz,  $\text{NCH}_2$ ), 6.55–6.70 (m, 2H, aryl-CH, dmba), 6.90–7.05 (m, 2H, aryl-CH, dmba), 7.50–7.60 (m, 4H, *m*-aryl,  $\text{PPh}_2$ ), 7.60–7.70 (m, 2H, *p*-aryl,  $\text{PPh}_2$ ), 7.85–8.00 (m, 4H, *o*-aryl,  $\text{PPh}_2$ ).  $^{13}\text{C}\{^1\text{H}\}$  NMR ( $\text{CD}_2\text{Cl}_2$ ):  $\delta$  25.9 (d,  $^3J_{\text{P-C}} = 7.5$  Hz,  $\text{C(O)CH}_3$ ), 30.7 (s,  $\text{CH}_2$ , THT), 39.8 (br s,  $\text{SCH}_2$ , THT), 49.9 (d,  $^3J_{\text{P-C}} = 2.7$  Hz,  $\text{N(CH}_3)_2$ ), 70.6 (d,  $^{3+4}J_{\text{P-C}} = 3.4$  Hz,  $\text{NCH}_2$ ), 123.4 (s, aryl, dmba), 125.1 (s, aryl, dmba), 126.3 (d,  $J_{\text{P-C}} = 5.5$  Hz, aryl, dmba), 129.3 (d,  $^3J_{\text{P-C}} = 11.2$  Hz, *m*-aryls,  $\text{PPh}_2$ ), 131.0 (d,  $^1J_{\text{P-C}} = 57.7$  Hz, *ipso*-aryls,  $\text{PPh}_2$ ), 132.7 (d,  $^4J_{\text{P-C}} = 2.5$  Hz, *p*-aryls,  $\text{PPh}_2$ ), 133.4 (d,  $^2J_{\text{P-C}} = 13.6$  Hz, *o*-aryls,  $\text{PPh}_2$ ), 137.6 (d,  $J_{\text{P-C}} = 10.6$  Hz, aryl, dmba), 145.0 (s,  $\text{C}_q\text{-dmba}$ ), 149.4 (d,  $J_{\text{P-C}} = 1.8$  Hz,  $\text{C}_q\text{-dmba}$ ), 187.7 (d,  $^{2+3}J_{\text{P-C}} = 4.9$  Hz, CO); the  $\text{CF}_3$  of OTf could not be assigned.  $^{19}\text{F}\{^1\text{H}\}$  NMR ( $\text{CD}_2\text{Cl}_2$ ):  $\delta$  -79.2 (s, OTf).  $^{31}\text{P}\{^1\text{H}\}$  NMR ( $\text{CD}_2\text{Cl}_2$ ):  $\delta$  92.7 (s,  $\text{PPh}_2$ ).  $^{31}\text{P}\{^1\text{H}\}$  NMR ( $\text{CDCl}_3$ ):  $\delta$  92.7 (s,  $\text{PPh}_2$ ). IR (KBr, select.):  $\nu(\text{NC+CO})$  1509  $\text{cm}^{-1}$ . Anal. Calcd for  $\text{C}_{23}\text{H}_{33}\text{AuF}_3\text{N}_2\text{O}_4\text{PPdS}_2$  (917.06): C, 36.67; H, 3.63; N, 3.05. Found: C, 36.90; H, 3.94; N, 2.89.

**Method B.** A solution of  $[\{\text{Ag}(\text{2})\text{OTf}\}]_n$ , prepared in situ by addition of solid  $\text{AgOTf}$  (0.09 g, 0.35 mmol) to a solution of **2** (0.17 g, 0.36 mmol) in THF (15 mL) and stirring for 2 h at room temperature, was filtered into a solution of  $[\text{AuCl}(\text{THT})]$  (0.11 g, 0.11 mmol) in THF (15 mL). An off-white precipitate was formed immediately, and the mixture was stirred for 2 h. After removing all volatiles in vacuo, the composition of the residue was controlled by  $^{31}\text{P}\{^1\text{H}\}$  NMR spectroscopy and the phosphorus-containing fragments **7<sup>+</sup>** and **8<sup>+</sup>** were found in a ratio 1:1, respectively.  $^{31}\text{P}\{^1\text{H}\}$  NMR ( $\text{CDCl}_3$ ):  $\delta$  92.7 (s,  $\text{PPh}_2$  in **7<sup>+</sup>**), 94.1 (s,  $\text{PPh}_2$  in **8<sup>+</sup>**).

**Method C.** THT (2 mL) and solid  $\text{AgOTf}$  (0.12 g, 0.47 mmol) were added to a solution of **6** (0.33 g, 0.46 mmol) in  $\text{CH}_2\text{Cl}_2$  (15 mL). An off-white precipitate was formed immediately, and the mixture was stirred for 1 h at room temperature. After removing all volatiles in vacuo, the composition of the residue was controlled by  $^{31}\text{P}\{^1\text{H}\}$  NMR spectroscopy and three phosphorus-containing fragments were found in a ratio 2:4:1, respectively.  $^{31}\text{P}\{^1\text{H}\}$  NMR ( $\text{CD}_2\text{Cl}_2$ ):  $\delta$  48.7 (s, unidentified product), 92.5 (s,  $\text{PPh}_2$  in **7<sup>+</sup>**), 94.1 (s,  $\text{PPh}_2$  in **8<sup>+</sup>**).

**Preparation and Spectroscopic Data for  $[\{\text{Pd}(\text{dmba})(\kappa^2\text{-P,O-PPh}_2\text{NC(O)Me})\}\text{Au}(\text{tth})\text{BF}_4]$  (**7-BF<sub>4</sub>**).** A solution of  $[\text{Au}(\text{THT})]\text{BF}_4$ , prepared in situ at -60 °C by addition of solid  $\text{AgBF}_4$  (0.13 g, 0.67 mmol) to a solution of  $[\text{AuCl}(\text{THT})]$  (0.20 g, 0.63 mmol) in  $\text{CH}_2\text{Cl}_2$  (15 mL), was filtered at -60 °C via cannula into a solution of **2** (0.30 g, 0.62 mmol) in THF (25 mL). An off-white precipitate was formed immediately, and the mixture was stirred for 2 h while slowly reaching room temperature. After removing all volatiles in vacuo, the composition of the residue was controlled by  $^{31}\text{P}\{^1\text{H}\}$  NMR spectroscopy and three phosphorus-containing fragments were found in a 1:1:1 ratio.  $^{31}\text{P}\{^1\text{H}\}$  NMR ( $\text{CDCl}_3$ ):  $\delta$  80.3 (s,  $\text{PPh}_2$  in **5<sup>+</sup>**), 92.6 (s,  $\text{PPh}_2$  in **7<sup>+</sup>**), 94.1 (s,  $\text{PPh}_2$  in **8<sup>+</sup>**).

(16) Kuhlmann, K.; Grant, D. M. *J. Phys. Chem.* **1964**, *68*, 3208.

(17) Uson, R.; Laguna, A.; Laguna, M. *Inorg. Synth.* **1989**, *26*, 85.

(18) Kubas, G. J. *Inorg. Synth.* **1979**, *19*, 90.

**Table 2. Selected Crystallographic Data for Complexes 2, 5·OTf, 6, 7·BF<sub>4</sub>, 8·BF<sub>4</sub>·2CH<sub>2</sub>Cl<sub>2</sub>, and 9·BF<sub>4</sub>**

	<b>2</b>	<b>5·OTf</b>	<b>6</b>	<b>7·BF<sub>4</sub></b>	<b>8·BF<sub>4</sub>·2CH<sub>2</sub>Cl<sub>2</sub></b>	<b>9·BF<sub>4</sub></b>
formula	C <sub>23</sub> H <sub>25</sub> N <sub>2</sub> OPPd	C <sub>23</sub> H <sub>26</sub> N <sub>2</sub> OPPd, CF <sub>3</sub> SO <sub>3</sub>	C <sub>23</sub> H <sub>25</sub> AuClN <sub>2</sub> OP Pd	C <sub>27</sub> H <sub>33</sub> AuN <sub>2</sub> OP Pd S, BF <sub>4</sub>	C <sub>46</sub> H <sub>50</sub> AuN <sub>4</sub> O <sub>2</sub> P <sub>2</sub> Pd <sub>2</sub> BF <sub>4</sub> 2(CH <sub>2</sub> Cl <sub>2</sub> )	C <sub>46</sub> H <sub>50</sub> CuN <sub>4</sub> O <sub>2</sub> P Pd <sub>2</sub> , BF <sub>4</sub>
fw	482.82	632.90	715.24	854.76	1419.27	1115.99
cryst syst	monoclinic	triclinic	triclinic	monoclinic	triclinic	monoclinic
space group	<i>P</i> 2 <sub>1</sub> / <i>n</i>	<i>P</i> $\bar{1}$	<i>P</i> $\bar{1}$	<i>P</i> 2 <sub>1</sub> / <i>c</i>	<i>P</i> $\bar{1}$	<i>P</i> 2 <sub>1</sub> / <i>n</i>
<i>a</i> (Å)	9.105(1)	9.258(1)	9.2940(2)	9.7620(2)	10.0860(1)	12.130(2)
<i>b</i> (Å)	24.945(5)	10.199(1)	11.4570(2)	19.4120(5)	13.2050(2)	18.709(3)
<i>c</i> (Å)	9.626(1)	14.834(2)	11.6150(3)	15.5880(4)	21.2590(3)	20.621(3)
$\alpha$ (deg)	90	80.986(5)	86.9000(8)	90	90.27(5)	90
$\beta$ (deg)	99.16(5)	73.696(5)	80.4300(7)	98.5530(9)	92.78(4)	90.93(5)
$\gamma$ (deg)	90	78.136(5)	72.980(1)	90	99.31(9)	90
<i>V</i> (Å <sup>3</sup> )	2158.4(5)	1308.3(3)	1166.14(4)	2921.1(1)	2790.6(7)	4679(1)
<i>Z</i>	4	2	2	4	2	4
cryst size (mm <sup>3</sup> )	0.15 × 0.13 × 0.09	0.10 × 0.09 × 0.08	0.10 × 0.09 × 0.08	0.03 × 0.02 × 0.01	0.10 × 0.09 × 0.08	0.08 × 0.07 × 0.05
color	yellow	colorless	colorless	yellow	colorless	colorless
<i>D</i> <sub>calc</sub> (g·cm <sup>-3</sup> )	1.486	1.607	2.037	1.944	1.689	1.584
$\mu$ (mm <sup>-1</sup> )	0.949	0.905	7.255	5.808	3.562	1.337
<i>T</i> (K)	173(2)	173(2)	293(2)	173(2)	173(2)	173(2)
<i>F</i> (000)	984	640	684	1656	1392	2248
$\theta$ limits (deg)	1.63/30.01	1.44/27.87	1.78/30.04	1.69/30.02	1.82/30.03	1.47/29.95
no. of data measd	6011	6204	6789	8529	16 323	13 529
no. of data ( <i>I</i> > 2 $\sigma$ ( <i>I</i> ))	4249	5087	5936	4259	11 545	8539
no. of params	253	329	271	352	610	559
<i>R</i> <sub>1</sub>	0.0404	0.0355	0.0323	0.0546	0.0492	0.0803
<i>wR</i> <sub>1</sub>	0.1290	0.0814	0.1127	0.1614	0.1430	0.1449
GOF	1.177	1.057	1.062	0.969	0.987	1.104
max./min. res dens (e·Å <sup>-3</sup> )	0.610/−0.868	0.505/−0.958	1.375/−2.913	1.127/−1.153	1.435/−1.267	1.008/−0.710

Single crystals of 7·BF<sub>4</sub> suitable for X-ray diffraction were obtained by layering a CDCl<sub>3</sub> solution with pentane.

**Preparation and Spectroscopic Data for [(Pd(dmba)(κ<sup>2</sup>-P,O-PPh<sub>2</sub>NC(O)Me)<sub>2</sub>Au]BF<sub>4</sub> (8·BF<sub>4</sub>).** A solution of [Au-(THT)]BF<sub>4</sub>, prepared in situ at −60 °C by addition of solid AgBF<sub>4</sub> (0.06 g, 0.31 mmol) to a solution of [AuCl(THT)] (0.10 g, 0.31 mmol) in CH<sub>2</sub>Cl<sub>2</sub> (15 mL), was filtered at −60 °C via cannula into a solution of 2 (0.30 g, 0.62 mmol) in THF (25 mL). An off-white precipitate was formed immediately, and the mixture was stirred for 3 h while slowly reaching room temperature. After removing all volatiles in vacuo, the residue was washed with THF (2 × 5 mL) and dried again in vacuo to yield an off-white powder, which was found to be the desired product as CH<sub>2</sub>Cl<sub>2</sub> adduct (0.32 g, 0.24 mmol, 77%). Single crystals suitable for X-ray diffraction were obtained by layering a CH<sub>2</sub>Cl<sub>2</sub> solution with pentane. <sup>1</sup>H NMR (CDCl<sub>3</sub>): δ 1.90 (d, 2 × 3H, <sup>4</sup>J<sub>P-H</sub> = 0.6 Hz, C(O)CH<sub>3</sub>), 2.86 (d, 2 × 6H, <sup>4</sup>J<sub>P-H</sub> = 2.6 Hz, N(CH<sub>3</sub>)<sub>2</sub>), 3.97 (d, 2 × 2H, <sup>4</sup>J<sub>P-H</sub> = 2.1 Hz, NCH<sub>2</sub>), 5.30 (s, 2H, CH<sub>2</sub>Cl<sub>2</sub>), 6.45–6.55 (m, 2 × 1H, aryl-CH, dmba), 6.60–6.70 (m, 2 × 1H, aryl-CH, dmba), 6.85–7.00 (m, 2 × 2H, aryl-CH, dmba), 7.40–7.50 (m, 2 × 4H, *m*-aryl, PPh<sub>2</sub>), 7.55–7.65 (m, 2 × 2H, *p*-aryl, PPh<sub>2</sub>), 7.70–7.80 (m, 2 × 4H, *o*-aryl, PPh<sub>2</sub>). <sup>13</sup>C{<sup>1</sup>H} NMR (CDCl<sub>3</sub>): δ 25.4 (d, <sup>3</sup>J<sub>P-C</sub> = 7.6 Hz, C(O)CH<sub>3</sub>), 50.1 (d, <sup>3</sup>J<sub>P-C</sub> = 2.8 Hz, N(CH<sub>3</sub>)<sub>2</sub>), 53.5 (CH<sub>2</sub>Cl<sub>2</sub>), 70.7 (d, <sup>3+4</sup>J<sub>P-C</sub> = 2.8 Hz, NCH<sub>2</sub>), 123.3 (s, aryls, dmba), 125.1 (s, aryls, dmba), 126.3 (d, *J*<sub>P-C</sub> = 5.5 Hz, aryls, dmba), 129.2 (d, <sup>3</sup>J<sub>P-C</sub> = 11.1 Hz, *m*-aryls, PPh<sub>2</sub>), 130.7 (d, <sup>1</sup>J<sub>P-C</sub> = 61.1 Hz, *ipso*-aryls, PPh<sub>2</sub>), 132.4 (d, <sup>4</sup>J<sub>P-C</sub> = 2.8 Hz, *p*-aryls, PPh<sub>2</sub>), 133.4 (d, <sup>2</sup>J<sub>P-C</sub> = 13.8 Hz, *o*-aryls, PPh<sub>2</sub>), 137.6 (d, *J*<sub>P-C</sub> = 10.4 Hz, aryls, dmba), 145.4 (d, *J*<sub>P-C</sub> = 1.4 Hz, aryls, C<sub>q</sub>-dmba), 149.1 (d, *J*<sub>P-C</sub> = 1.4 Hz, aryls, C<sub>q</sub>-dmba), 187.6 (s, CO). <sup>19</sup>F{<sup>1</sup>H} NMR (CDCl<sub>3</sub>): δ −154.4 (s, BF<sub>4</sub>). <sup>31</sup>P{<sup>1</sup>H} NMR (CDCl<sub>3</sub>): δ 94.1 (s, PPh<sub>2</sub>). IR (KBr, select.): ν(NC+CO) 1508 s cm<sup>-1</sup>. Anal. Calcd for C<sub>46</sub>H<sub>50</sub>-AuBF<sub>4</sub>N<sub>4</sub>O<sub>2</sub>P<sub>2</sub>Pd<sub>2</sub>·CH<sub>2</sub>Cl<sub>2</sub> (1334.41): C, 42.30; H, 3.93; N, 4.20. Found: C, 41.85; H, 4.04; N, 4.13.

**Preparation and Spectroscopic Data for [(Pd(dmba)(κ<sup>2</sup>-P,O-PPh<sub>2</sub>NC(O)Me)<sub>2</sub>Cu]BF<sub>4</sub> (9·BF<sub>4</sub>).** Solid 2 (0.31 g, 0.64 mmol) was dissolved in THF (25 mL), and [Cu(NCMe)<sub>4</sub>]BF<sub>4</sub> (0.10 g, 0.32 mmol) was added in one portion. A white precipitate was formed after 5 min, and the mixture was stirred for 2 h. After filtration, the residue was washed with THF (5 mL) and dried in vacuo to yield the product as a colorless powder (0.31 g, 0.28 mmol, 88%). Single crystals suitable for X-ray diffraction were obtained by layering a CH<sub>2</sub>Cl<sub>2</sub> solution with pentane. <sup>1</sup>H NMR (CDCl<sub>3</sub>): δ 1.80 (s, 2 × 3H, C(O)CH<sub>3</sub>), 2.84 (d, 2 × 6H, <sup>4</sup>J<sub>P-H</sub> = 2.5 Hz, N(CH<sub>3</sub>)<sub>2</sub>), 3.95 (d, 2 × 2H, <sup>4</sup>J<sub>P-H</sub> = 1.9 Hz, NCH<sub>2</sub>), 6.50–6.55 (m, 2 × 1H, aryl-CH, dmba), 6.60–6.70 (m, 2 × 1H, aryl-CH, dmba), 6.90–7.00 (m, 2 × 2H, aryl-CH, dmba), 7.35–7.45 (m, 2 × 4H, *m*-aryl, PPh<sub>2</sub>), 7.50–7.60 (m, 2 × 2H, *p*-aryl, PPh<sub>2</sub>), 7.60–7.70 (m, 2 × 4H, *o*-aryl, PPh<sub>2</sub>). <sup>13</sup>C{<sup>1</sup>H} NMR (CDCl<sub>3</sub>): δ 24.9 (d, <sup>3</sup>J<sub>P-C</sub> = 9.3 Hz, C(O)CH<sub>3</sub>), 50.1 (d, <sup>3</sup>J<sub>P-C</sub> = 2.4 Hz, N(CH<sub>3</sub>)<sub>2</sub>), 70.7 (d, <sup>3+4</sup>J<sub>P-C</sub> = 3.2 Hz, NCH<sub>2</sub>), 123.2 (s, aryls, dmba), 125.0 (s, aryls, dmba), 126.2 (d, *J*<sub>P-C</sub> = 5.2 Hz, aryls, dmba), 129.3 (d, <sup>3</sup>J<sub>P-C</sub> = 11.3 Hz, *m*-aryls, PPh<sub>2</sub>), 131.3 (d, <sup>1</sup>J<sub>P-C</sub> = 57.7 Hz, *ipso*-aryls, PPh<sub>2</sub>), 132.3 (d, <sup>4</sup>J<sub>P-C</sub> = 2.0 Hz, *p*-aryls, PPh<sub>2</sub>), 133.1 (d, <sup>2</sup>J<sub>P-C</sub> = 13.4 Hz, *o*-aryls, PPh<sub>2</sub>), 137.6 (d, *J*<sub>P-C</sub> = 10.2 Hz, aryls, dmba), 145.5 (s, aryls, C<sub>q</sub>-dmba), 149.1 (d, *J*<sub>P-C</sub> = 1.7 Hz, aryls, C<sub>q</sub>-dmba), 187.7 (d, <sup>2</sup>J<sub>P-C</sub> = 2.2 Hz, CO). <sup>19</sup>F{<sup>1</sup>H} NMR (CDCl<sub>3</sub>): δ −154.6 (s, BF<sub>4</sub>). <sup>31</sup>P{<sup>1</sup>H} NMR (CDCl<sub>3</sub>): δ 89.2 (s, PPh<sub>2</sub>). <sup>31</sup>P{<sup>1</sup>H} NMR (CD<sub>2</sub>Cl<sub>2</sub>): δ 89.0 (s, PPh<sub>2</sub>). IR (KBr, select.): ν(NC+CO) 1492 s cm<sup>-1</sup>. Anal. Calcd for C<sub>46</sub>H<sub>50</sub>-BCuF<sub>4</sub>N<sub>4</sub>O<sub>2</sub>P<sub>2</sub>Pd<sub>2</sub> (1116.06): C, 49.51; H, 4.52; N, 5.02. Found: C, 49.20; H, 4.75; N, 4.67.

**Reaction between [Pd(dmba)(κ<sup>2</sup>-P,O-PPh<sub>2</sub>NC(O)Me)] (2) and [Cu(NCMe)<sub>4</sub>]BF<sub>4</sub> to Yield 10·BF<sub>4</sub>.** Solid 2 (0.24 g, 0.50 mmol) was dissolved in THF (20 mL), and [Cu(NCMe)<sub>4</sub>]BF<sub>4</sub> (0.15 g, 0.48 mmol) was added in one portion. A white precipitate was formed after 5 min, and the mixture was stirred for 3 h. After removing the volatiles in vacuo, the



composition of the residue was controlled by  $^{31}\text{P}\{^1\text{H}\}$  NMR spectroscopy and three phosphorus-containing compounds were found in a 4:1:2 ratio, respectively.  $^{31}\text{P}\{^1\text{H}\}$  NMR ( $\text{CDCl}_3$ ):  $\delta$  80.3 (s,  $\text{PPh}_2$  in **5**<sup>+</sup>), 88.9 (s,  $\text{PPh}_2$  in **10**<sup>+</sup>), 89.2 (s,  $\text{PPh}_2$  in **9**<sup>+</sup>).

**Reaction between [Pd(dmba)( $\kappa^2$ -P,O-PPh<sub>2</sub>NC(O)Me)] (2) and [Pd(dmba)( $\kappa^2$ -P,O-PPh<sub>2</sub>NHC(O)Me)OTf] (5-OTf).** Solid **2** (0.12 g, 0.25 mmol) and **5-OTf** (0.16 g, 0.25 mmol) were dissolved in THF (20 mL) or  $\text{CH}_2\text{Cl}_2$ /toluene (20 mL), and the mixture was stirred for 1 h. After removing the solvent in vacuo, the composition of the residue was controlled by means of  $^{31}\text{P}\{^1\text{H}\}$  NMR spectroscopy. Analogously, the reaction can be done using **2** and **5-PF<sub>6</sub>**.  $^1\text{H}$  NMR ( $\text{CDCl}_3$ ):  $\delta$  2.34 (s, 2  $\times$  3H, C(O)CH<sub>3</sub>), 2.89 (d, 2  $\times$  6H,  $^4J_{\text{P-H}} = 2.6$  Hz, N(CH<sub>3</sub>)<sub>2</sub>), 4.00 (d, 2  $\times$  2H,  $^4J_{\text{P-H}} = 2.0$  Hz, NCH<sub>2</sub>), 6.60–6.70 (m, 2  $\times$  2H, aryl-CH, dmba), 6.90–7.05 (m, 2  $\times$  2H, aryl-CH, dmba), 7.40–7.60 (m, 2  $\times$  6H, *m*-, *p*-aryl, PPh<sub>2</sub>), 7.75–7.85 (m, 2  $\times$  4H, *o*-aryl, PPh<sub>2</sub>).  $^{31}\text{P}\{^1\text{H}\}$  NMR ( $\text{CDCl}_3$ ):  $\delta$  81.0 (s, PPh<sub>2</sub>).  $^{31}\text{P}\{^1\text{H}\}$  NMR ( $\text{CD}_2\text{Cl}_2$ ):  $\delta$  80.8 (s, PPh<sub>2</sub>).  $^{31}\text{P}\{^1\text{H}\}$  NMR ( $\text{CD}_2\text{Cl}_2$ , 181 K):  $\delta$  81.6 (s, PPh<sub>2</sub>), 83.6 (s, PPh<sub>2</sub>).

**X-ray Collection and Structure Determinations.** The diffraction data were collected on a Nonius Kappa-CCD area detector diffractometer (Mo K $\alpha$ ,  $\lambda = 0.71070$  Å; phi scan). The relevant data are summarized in Table 2. The cell parameters were determined from reflections taken from one set of 10 frames (1.0° steps in phi angle), each at 20 s exposure. The structures were solved using direct methods (SHELXS97) and refined against  $F^2$  using the SHELXL97 software. The absorp-

tion was corrected empirically (with Sortav) for compounds **2**, **6**, and **8**·BF<sub>4</sub>·2CH<sub>2</sub>Cl<sub>2</sub>.<sup>19</sup> All non-hydrogen atoms except those from CH<sub>2</sub>Cl<sub>2</sub> in **8**·BF<sub>4</sub>·2CH<sub>2</sub>Cl<sub>2</sub> were refined with anisotropic parameters. The hydrogen atoms were included in their calculated positions and refined with a riding model in SHELXL97.<sup>20</sup>

The crystallographic material can be obtained from the Cambridge Crystallographic Data Centre, 12 Union Road, Cambridge CB2 1EZ, UK (fax: (44) 1223-336-033; e-mail: deposit@ccdc.cam.ac.uk), under deposition numbers CCDC 261460–261465.

**Acknowledgment.** This work was supported by the CNRS and the Ministère de la Recherche. We are grateful to the European Commission for support in the COST D-30 Action and to a Marie Curie fellowship (HPMF-CT-2002-01659) and to the French Embassy in Berlin and the Ministère des Affaires Etrangères (Paris) for a postdoctoral grant to N.O.-W. The authors also wish to thank Anne Degrémont for experimental support.

**Supporting Information Available:** Crystallographic information files (CIF) and ORTEP plots of all the structures. This material is available free of charge via Internet at <http://pubs.acs.org>.

OM050156D

(19) Sheldrick, G. M. *SHELXL97*, Program for the refinement of crystal structures; University of Göttingen: Germany, 1997.

(19) Blessing, R. H. *Crystallogr. Rev.* **1987**, *1*, 3.